

## Research Article

# Design of a Versatile and Low Cost $\mu$ Volt Level A to D Conversion System for Use in Medical Instrumentation Applications

Kerry Williams and Neil Robinson

*School of Applied Sciences, RMIT University, Melbourne, Victoria 3000, Australia*

Correspondence should be addressed to Kerry Williams, [kerry.williams@rmit.edu.au](mailto:kerry.williams@rmit.edu.au)

Received 27 November 2007; Revised 3 April 2008; Accepted 14 August 2008

Recommended by P.-C. Chung

Modern medical facilities place considerable reliance on electronic instrumentation for purposes of calibration and monitoring of therapeutic processes, many of which employ electrical and electronic apparatus that itself generates considerable levels of interference in the form of background electromagnetic radiation (EMR). Additionally diverse ambient conditions in the clinical environment such as uncontrolled temperature, humidity, noise, and vibration place added stress on sensitive instrumentation. In order to obtain accurate, repeatable, and reliable data in such environments, instrumentation used must be largely immune to these factors. Analogue instrumentation is particularly susceptible to unstable environmental conditions. Sensors typically output an analogue current or voltage and it can be demonstrated that considerable overall benefit to the measuring process would result if sensor outputs could be converted to a robust digital format at the earliest possible stage. A practical and low cost system for A to D conversion at  $\mu$ Volt signal levels is described in this work. It has been successfully employed in portable radiation dosimetry instrumentation and used under diverse clinical conditions and it affords an improvement in signal resolution in excess of an order of magnitude over commonly used analogue techniques.

Copyright © 2008 K. Williams and N. Robinson. This is an open access article distributed under the Creative Commons Attribution License, which permits unrestricted use, distribution, and reproduction in any medium, provided the original work is properly cited.

## 1. INTRODUCTION

Development of the instrument described in this paper was inspired by a requirement in our laboratories to measure X-ray fields using near tissue equivalent plastic organic scintillator materials as the sensor element. Under clinical conditions where beam energies in the KVp range are used, these sensors produce extremely low levels of light which when interfaced with the most sensitive of photodiodes yet only produce output currents in the nanoamp region.

When coupled with a well shielded buffer amplifier, this arrangement still only provides usable output levels of a few microvolts. The task of raising such signal levels to a point where adequate resolution could be achieved, plus the potential to capture and store the data, presented particular difficulties. Laboratory systems operated in a controlled environment can be effective for the measurement of medium to high level signals but may lack stability and resolution when very low signal levels are encountered

[1] and are generally costly and lack portability. Our research has resulted in the design and development of a practical and portable instrument which has been effectively applied in clinical dosimetry situations involving near tissue equivalent radiation dose measurements [2, 3]. Technical details outlining the practical implementation of the system are given below.

Analogue circuitry is readily affected by changes in ambient temperature, vibration, unexpected variations in power supply voltages, and the like. In many instances, interference levels from these sources and extraneous EMR generated by adjacent clinical equipment such as X-ray generators, linear accelerators, and general control and computing devices can readily exceed wanted signal levels by several orders of magnitude.

The ability to achieve reliable very low level analogue amplification in anything but controlled laboratory conditions presents a considerable challenge, and without a guaranteed level of performance and stability in front end

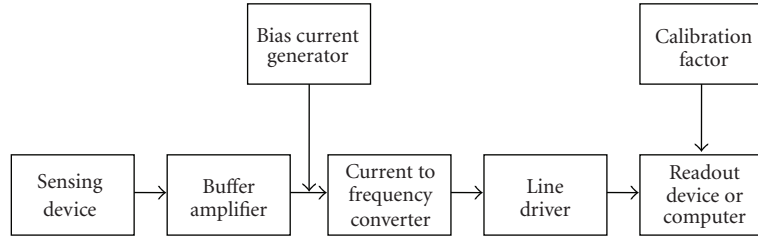


FIGURE 1: Block diagram showing overview of concept and signal processing chain.

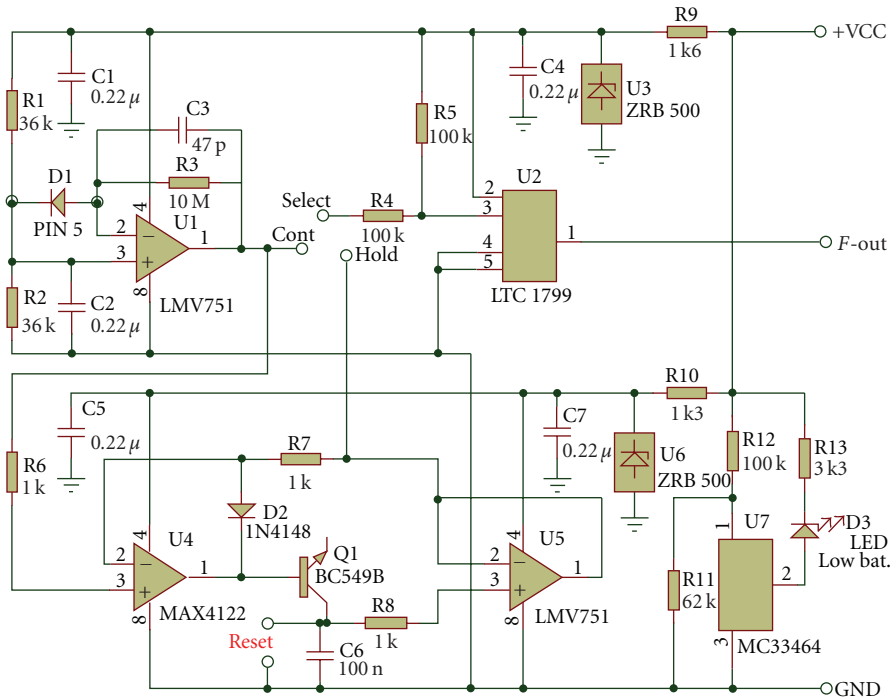


FIGURE 2: Schematic diagram of a prototype instrument used for scintillation counting.

stages, introduced errors and spurious responses will be indistinguishable from the desired signal once downstream conversion to a digital format has occurred.

Achieving reliable analogue amplification and filtering at the ultra low sensor outputs encountered proved to be unproductive in that every analogue stage produced and added its own levels of instability and self-generated noise to the degree that the wanted signal information was lost in the noise floor of the added circuitry. To overcome this limitation, the possibility of early conversion to a digital signal format was investigated, however it was found that system generated noise from available PC-based A to D converters, plus the high cost of multibit converters able to resolve signals at microvolt levels severely restricted the feasibility of such a proposal.

There being no suitable or affordable “off the shelf” system which could be adapted to the task, it was necessary to design and develop a novel technology that could directly interface a range of sensor elements and to provide a reliable and low cost method of capturing and storing the resultant data stream.

The technique developed and employed has been shown to markedly improve noise immunity of low level measuring instruments and also to offer considerable improvements to system stability under hostile environmental conditions where external interference and unpredictable shifts in environmental conditions are present.

## 2. CIRCUIT DESIGN CONSIDERATIONS

An integrated system of analogue-to-digital conversion at the microvolt level was proposed and developed as described below, for the specific purpose of direct coupling to a variety of sensors, and has been implemented using readily available low power integrated circuit technology. An overview of the concept is shown in Figure 1.

Applying this concept, the design and development of a practical electronic circuit was undertaken. A typical prototype schematic is shown in Figure 2 where it will be seen that the use of analogue circuitry has been reduced to the minimum required for correct termination of the sensing device employed. Analogue input signal currents to the first

stage device U2 can be less than a microamp and yet produce a reliable response.

The particular configuration shown in Figure 2 employs a photodiode sensor in an instrument intended to be used as a scintillation counter. The buffered voltage from the sensor is coupled via a resistance selected to provide the required level of current injection into pin 3 of U2. A bias current generator adds a fixed current to enable an appropriate baseline to be set. The functions of U4 and U5 are not part of the conversion process but have been added in this instance to provide a conventional sample and hold facility which, in the case of a hand-held instrument, allows for a “snapshot” of the data stream to be made manually at a time chosen by the operator. Use of this additional facility does not interrupt the data stream being processed and stored by an associated personal computer (PC). The base collector junction of Q1 is used for reverse voltage blocking and level shifting and could be replaced with a low leakage diode if desired. Device U7 is a battery condition indicator and may be omitted if the instrument is to be mains powered.

Once conversion from current-to-frequency has been performed by U1 and U2 the resulting logic level data stream, which has a pulse rate directly proportional to the electrical output of the sensor, is passed to a line drive circuit U8 (not shown). The low output impedance of this device is capable of direct connection to a readout device such as frequency meter or pulse counter, or of driving tens of metres of coaxial cable for remote connection to a PC or data logger where further analysis and storage of measurement data can occur.

The change in output frequency bears a linear relationship to the magnitude of the sensed phenomena, thus it is only necessary to include an appropriate calibration factor in order to provide automatic interpretation of the output pulse train and to offer a direct readout in the numerical units desired. In the case of PC-based data storage, a simple algorithm and graphing software may be used to provide a direct scaled onscreen display.

Employing modern low power surface mount components to conserve space and to enhance battery life, a National Semiconductor LMV 751 [4] low voltage operational amplifier is used as the buffer stage required to interface the detector, in this case a precision photodiode, UDT Sensors PIN 5DPI, with a current-to-frequency converter.

It is important to keep the gain of this analogue stage to a minimum as it is the primary source of circuit generated noise. In practice it has been shown that a gain of ten combined with its impedance matching function is adequate, although gains of up to 40 have been used effectively where minute signal levels need to be accommodated.

Output from this stage is coupled through a 10 k $\Omega$  or 100 k $\Omega$  precision resistor (R4) to set the required conversion gain and thence to the current injection input of current controlled oscillator U2.

The DC supply for the circuit comprises a 9-volt battery regulated down to 5 volt by the use of a temperature compensated, surface mount bandgap reference device. This supplies a highly stable +5 volt to the active devices. The very low current drain of the circuit allows the use of this

ultrastable and low noise method of regulation, in preference to the considerably less precise commonly employed three-terminal voltage regulator integrated circuit.

The output signal characteristics of U2, in this case an LTC 1799 [5], are a considerable improvement over the older industry standard LM 331N devices and are compatible with typical logic level specifications. No further waveform processing is required between this point and the frequency counter unless a remote monitoring facility is required. In this case, normal instrumentation practice calls for a conventional cable driver stage to be added in order to preserve waveform integrity and device stability when driving the reactive elements of a long run of coaxial cable.

### 3. SIGNAL RESOLUTION

To establish resolution, accuracy, and repeatability of measurements it was necessary to quantify the level of residual noise from the analogue stage plus its stability over time, as any drift in the DC bias level arising from the buffer stage would be additive and indistinguishable from the wanted input signal. A UDT PIN 5DPI precision photodiode was used as a sensor during these tests and measurements. The data obtained was then used to establish the sensitivity and margins of uncertainty in the current-to-frequency conversion process.

A precise reference level used to establish the base frequency of the current-to-frequency converter stage was generated using a high-precision temperature compensated laboratory standard which may be regarded as sufficiently stable for the purposes of providing a reference current source for the instrument. After an initial warmup period of 15 minutes to obtain thermal equilibrium of the circuits inside the sealed instrument case, measurement of voltage from the buffer stage to a 10 000  $\Omega$  input resistor to the current-to-frequency converter was made using a precision data acquisition system having a base resolution of 100  $\mu$ V.

During this test no light was allowed to reach the photodiode. Bearing in mind the adequate but limiting factor of the 100  $\mu$ V resolution for the measuring equipment, the input voltage noise floor and drift of the instrument's input stages were logged and the results are shown graphically in Figures 3 and 4 below. These noise voltages are related to the input current to the current-to-frequency converter stage by the function  $E(t) = 10\,000I(t)$ .

Figure 3 shows the low level of baseline drift of about 19 Hz/min. after initial component thermal stability has been attained. This represents a level of output signal drift in the order of 0.02% per minute. Since most clinical measurements may be taken over durations shorter than a minute, this level of drift would not be significant.

The horizontal bands evident in Figure 4 are an artefact of the lower limit of resolution (100  $\mu$ V) achievable from the data acquisition system used in capturing this information and are not in any way a function of the buffer or frequency conversion. It can be seen that the characteristic of the total circuit and incidental noise is random with a worst-case peak to peak spread of 3.87 mV. As the negative and positive excursions are relatively uniform about a mean,

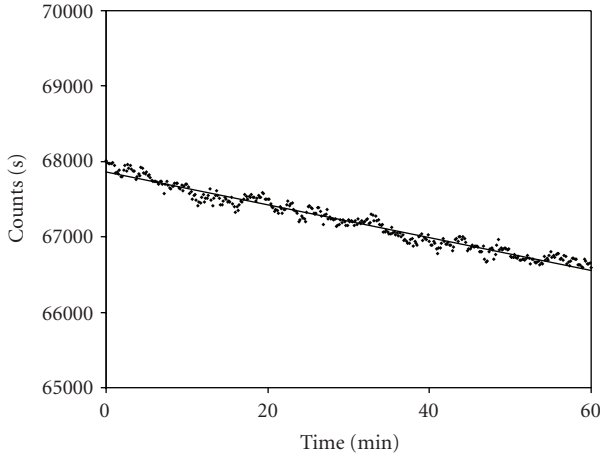


FIGURE 3: Baseline drift over a period of one hour after thermal stability achieved.

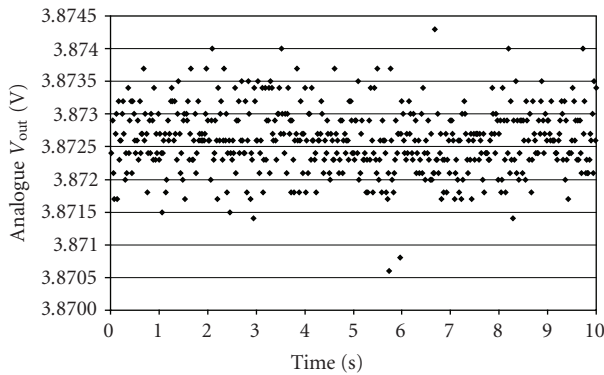


FIGURE 4: Noise measurements at output from analogue stage  $V_{out}$  versus. Time. 10 second recording at 50 Hz sample rate (500 readings). Note: Output voltage from the analogue buffer stage = 3.8726 V which comprises A/D converter bias voltage plus averaged noise voltage component,  $E(t)$ . Uncertainty (95% confidence limits) =  $\pm 44 \mu\text{V}$  when measured over a 10 s period. Noise Band (Worst Case): 3.7 mV (i.e.,  $\pm 1.85 \text{ mV}$ ).

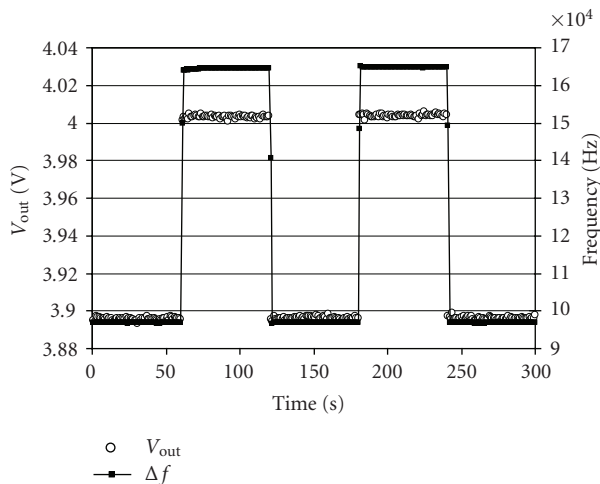


FIGURE 5:  $V_{out}$  from buffer stage versus frequency shift for  $\Delta V_{out} = 107.6 \text{ mV}$ .

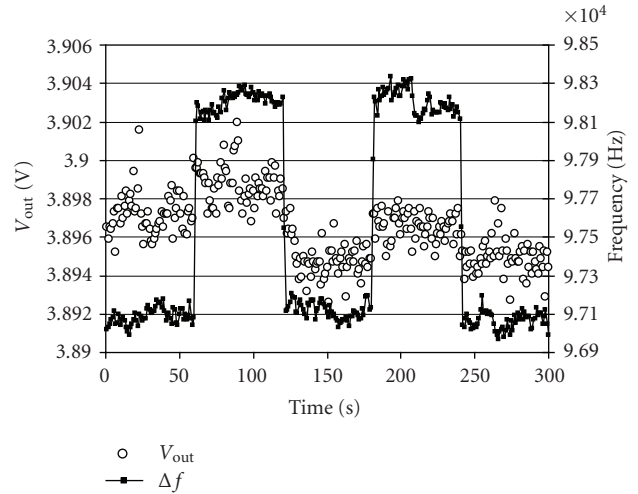


FIGURE 6:  $V_{out}$  from analogue buffer stage versus. Frequency shift for  $\Delta V_{out} = 2.0 \text{ mV}$ .

it can be shown that using the time averaging feature which is an inherent in the current-to-frequency conversion process the random negative and positive excursions of the noise component superimposed on the bias voltage which establishes the baseline are cancelled. Thus the bias voltage can, when monitored over a 10 second period, be determined to an accuracy of  $\pm 44 \mu\text{V}$ .

It can be seen from the data shown in Figure 4 that the noise floor of the electronic system, equivalent to an output of 3.87 mV peak to peak from the analogue buffer stage, will be the overall limiting factor for the resolution of the instrument. The following tests demonstrate that with the benefit of the time averaging feature inherent in this design, and utilising a conservative gain figure of 20x from the buffer stage, this equates to a minimum resolution of  $44 \mu\text{V}$ . or a sensor delta  $V$  output in the order of  $2.2 \mu\text{V}$ .

Using a very low level light source interfaced with the photodiode, a series of measurements were taken. Data logging over a number of 5 minute intervals while toggling the light source on and off for periods of 1 minute resulted in a series of graphs of the type shown in Figures 5 and 6.

Figure 5 shows the case when applying a reasonably high level signal,  $\Delta V_{out} = 107.6 \text{ mV}$ ,  $\Delta f = 67.753 \text{ kHz}$ . In this case, high levels of accuracy are available and the time integration effects which are inherent in this design play only a small part in defining resolution.

However in the example shown in Figure 6 signal input level is set at  $\Delta V_{out} = 2.0 \text{ mV}$ ,  $\Delta f = 1.117 \text{ kHz}$ , a point just above the minimum resolvable level of the noise floor of the analogue stage, and shows that a stable output frequency can still be obtained due to time integration which occurs in the current-to-frequency conversion stage.

Using the system described, data was tabulated comparing voltage output of the analogue buffer with the resulting frequency shift of the output of the current-to-frequency converter. Readings were taken at intervals from a level of 2 mV, which is approaching the noise floor of the stage, up to about 100 mV. The results are shown in Table 1, are plotted

TABLE 1: Analogue output and corresponding frequency shift from A/D conversion using a low level light source into a PIN 5DPI photodiode. Note the significant improvements in uncertainty factors after processing. (column 4)

Analogue $V_{out}$ (mV)	% ncertainty	I-F Frequency Shift (kHz)	% Uncertainty
$2.0 \pm 0.4$	20.0	$1.117 \pm 0.017$	1.5
$4.2 \pm 0.4$	9.5	$2.469 \pm 0.021$	0.85
$20.1 \pm 0.7$	3.5	$11.624 \pm 0.016$	0.14
$45.5 \pm 0.8$	1.8	$27.112 \pm 0.037$	0.14
$78.3 \pm 0.5$	0.64	$48.753 \pm 0.023$	0.05
$107.6 \pm 0.3$	0.28	$67.753 \pm 0.045$	0.07

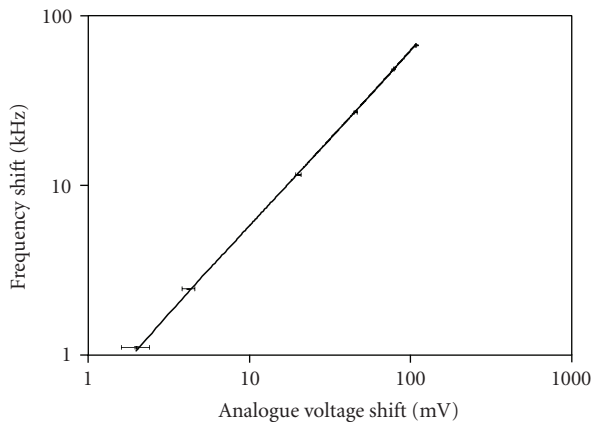


FIGURE 7: Graph of output Frequency versus. Analogue Voltage output from buffer. Note that this gives a sensitivity of  $0.631 \text{ kHz/mV}$  =  $631 \text{ Hz/mV}$ .

graphically in Figure 7, and describe a response curve for the instrument.

The numbers plotted in Table 1 readily reveal the improvement in reliability of data obtained after conversion. For example, at a 2 mV signal the level of uncertainty achievable from reading the buffer analogue output is 20% (an unacceptable error figure for any scientific instrument) whereas due to the significant noise immunity and resolving power provided by this unique digital conversion process the potential error is reduced to 1.5%.

As anticipated, the response of the electronic systems is fundamentally linear over its intended output range.

Hence it becomes simply a matter of calibrating frequency shift observed against a number of reference points for the source being measured, be it radiation, light, sound, temperature, magnetic flux and so forth. The range of measurements is limited only by the selection of transducer connected to the input buffer amplifier.

An instrument designed and constructed as described has been used to measure and profile the beta radiation from an Sr-90 brachytherapy source and was found to be particularly easy to use and to provide stable and repeatable results [3]. Due to the high sensitivity available from the instrument, it was possible to use a very small

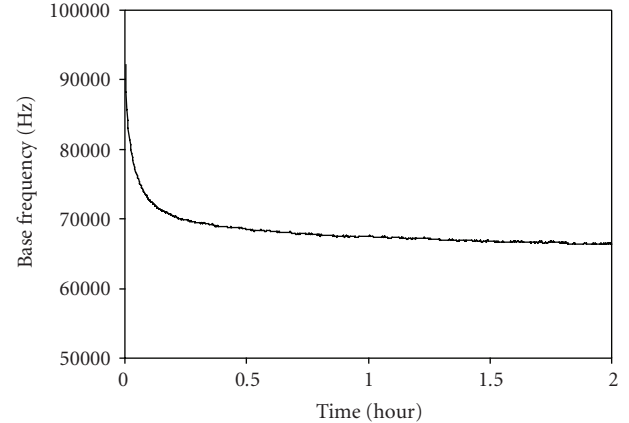


FIGURE 8: Drift over 2 hour period showing baseline stability attainable after 15 minutes initial warm-up period.

detection element and thereby to achieve submillimetre spatial resolution across the radiation field.

In applications where a differential input is appropriate for the type of sensor selected, the input Integrated Circuit LM751 may be replaced with a single AD626 [6] precision instrumentation differential amplifier. This change offers the advantages of enhanced common mode rejection and a reduction in device generated noise but at somewhat increased cost. Bench testing of a bread-boarded circuit using this concept resulted in an input stage that also achieved a considerably improved level of thermal and environmental immunity, resulting in the excellent baseline stability over time shown in Figure 8.

As would be expected overall stability and resolution are improved by adopting a differential input configuration and this would be the arrangement of choice where one side of the sensor was not inherently committed to ground, as is often the case in practice.

#### 4. CONCLUSION

The novel signal processing system described offers a high level of immunity to environmental EMR and internal circuit generated noise and furnishes a compact and low cost method for the capture and integrated digital processing of measurement data in a range of situations including clinical diagnostic and treatment venues.

The technique has been shown to give an improvement in signal resolution of at least an order of magnitude over typical analogue instrumentation and PC bus based A-D converters. The compact nature and low power consumption of the circuitry make the system eminently suitable for use in portable battery-operated instruments, in addition to its potential for incorporation into laboratory instrumentation where the effects of high levels of environmental noise and interference need to be neutralised. Under clinical conditions, the system has been successfully employed in a number of cases where low level radiation detection and measuring procedures were required.

Coupled with an organic plastic scintillation element for detection and measurement of X rays, a prototype instrument incorporating this method of signal capture and processing has been found to be particularly effective in providing direct readout of high intensity photon beams generated by clinical linear accelerators in situations involving high levels of background radiation and interference and where remote monitoring at distances of up to 30 metres from the detector has been required.

## REFERENCES

- [1] M. A. Clift, R. A. Sutton, and D. V. Webb, "Water equivalence of plastic organic scintillators in megavoltage radiotherapy bremsstrahlung beams," *Physics in Medicine and Biology*, vol. 45, no. 7, pp. 1885–1895, 2000.
- [2] K. Williams, N. Robinson, J. Trapp, et al., "A portable organic plastic scintillator dosimetry system for low energy X-rays: a feasibility study using an intraoperative X-ray unit as the radiation source," *Journal of Medical Physics*, vol. 32, no. 2, pp. 73–76, 2007.
- [3] M. Geso, N. Robinson, W. Schumer, and K. Williams, "Use of water-equivalent plastic scintillator for intravascular brachytherapy dosimetry," *Australasian Physical & Engineering Sciences in Medicine*, vol. 27, no. 1, pp. 5–10, 2004.
- [4] <http://www.national.com/catalog/>.
- [5] <http://www.linearteck.com/>.
- [6] <http://www.analog.com/product>.